

# Wafer Thickness, Texture and Performance of Multicrystalline Silicon Solar Cells.

C.J.J. Tool<sup>1</sup>, P. Manshanden, A.R. Burgers, A.W. Weeber

ECN - Solar Energy, PO Box 1, 1755 ZG Petten, The Netherlands

<sup>1</sup> telephone: +31 226 56 4135, fax +31 226 56 8214, email: tool@ecn.nl

## Abstract

The influence of wafer thickness and surface texturing of silicon solar cells on cell results has been investigated using neighbouring multicrystalline silicon wafers with thickness ranging from 150  $\mu\text{m}$  to 350  $\mu\text{m}$  and isotropic NaOH or acid etched. It was found experimentally that  $V_{oc}$  decreases nearly 1.5 % and  $J_{sc}$  decreases nearly 3 %, resulting in a 4 % relative decrease in efficiency, in halving the wafer thickness. These trends are independent of the front surface texturing.

Front surface texturing, however, results in a 6 % increase of  $J_{sc}$  and a nearly 6 % increase in efficiency independent of the wafer thickness.

Keywords: texturing, wafer thickness, rear reflection, BSF

## 1. Introduction

Two main issues concerning the use of thinner wafers are process yield and efficiency of the produced cells. In this paper we focus on efficiency as a function of wafer thickness for multicrystalline Si because we are unable to investigate the yield. Handling in our process line is very different from handling in an industrial process line. BP Solar has shown that Cz wafers down to 140  $\mu\text{m}$  can be processed in an industrial environment without additional yield losses [1].

The effect of wafer thickness on cell efficiency has been modelled extensively. These modelling results are supported by experimental results on mono-crystalline wafers, which are mechanically or chemically thinned to the desired thickness [e.g. 2,3]. In this work we use multi-crystalline wafers specially sawed by Bayer so that the thickness of neighbouring wafers varied in steps of about 25  $\mu\text{m}$  (Figure 1).

We previously presented the influence of the wafer thickness in relation to material quality [4] on comparable material. In this work we present the effect of front surface texturing on the relation between wafer thickness and cell efficiency for mc-Si solar cells.

## 2. Experimental set up

Sets of silicon wafers have been processed by standard processing sequences using industrial techniques. Each set consisted initially of eight  $10 \times 10 \text{ cm}^2$  neighbour wafers. The thickness of the wafers before saw damage removal ranged from 150 to 350  $\mu\text{m}$  in 25  $\mu\text{m}$  steps.

Three different methods have been used to remove the saw damage: a standard NaOH etch (identified by NaOH throughout this work) and two isotropic acid etches (identified by acid texture-1 and acid texture-2 respectively) both resulting in textured surfaces but with different reflectivity. We were unable to use neighbouring wafers over the different groups, because the nearest neighbours belong to the same set. Therefore, we used alternating adjacent sets for the 3 different groups so small differences in material quality over the experimental wafers are levelled out (Figure 1). The saw damage removal was followed by the diffusion of a shallow emitter (sheet resistivity 60-65  $\Omega/\text{sq}$ ) in a belt furnace. The emitter diffusion was performed in a single run at the same time – temperature settings for all the groups. Despite this, the sheet resistance of the NaOH group was 65  $\Omega/\text{sq}$  compared to 60  $\Omega/\text{sq}$  for the acid etched groups due to differences in surface morphology. After phosphorus glass removal a SiN anti reflection coating was deposited. From other experiments it is known that the optimum SiN deposition parameters differ for NaOH etched wafers and acid etched wafers. We decided to use the deposition parameters which were optimised for the etching method used. Front side metalisation (Ag) and rear side metalisation (Al) were applied by screen printing and simultaneously fired in an IR belt-furnace. It is known that the wafer thickness has an effect on the optimum firing condition. However, to minimise the influence of the firing condition on mainly the Al-BSF, we decided to use only two firing conditions. One for wafers thinner than 250  $\mu\text{m}$ , the other for the rest of the wafers, irrespective of the front side texturing. A consequence of this choice is that

only intermediate fill factors have been realised. Therefore, the comparison between the three saw damage removal methods will focus on the effect of the wafer thickness on  $J_{sc}$  and  $V_{oc}$ . To measure the temperature profile of the firing step, a thermocouple was glued on an etched wafer. This wafer was given the firing treatment without being metallised. The temperature of the wafer was in situ monitored with a Datapaq system [5].

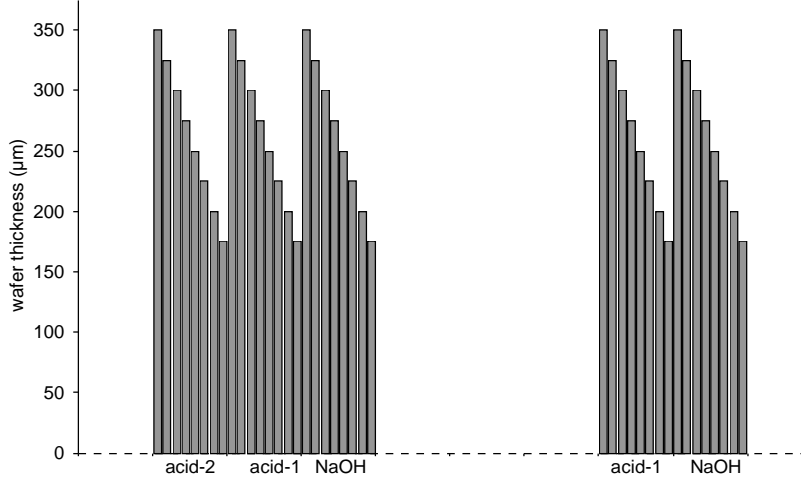


**Figure 1: wafer position in the ingot; distribution of the blocks over the 3 groups is also shown.**

We have measured the I-V characteristics of all cells according to ASTM-E948 norm using 2 current probes per busbar. The spectral response and the reflectance of selected cells have been measured to calculate the internal quantum efficiency IQE according to ASTM-1024 norm. The 95 % confidence limits are calculated using the computer program Statgraphics 5<sup>+</sup> [6]. To explain the observed trends device modelling was done with PC1D version 4.5 [7]. Although PC1D is a one-dimensional model, the observed trends of the various cell parameters are expected to be comparable to a more complicated two-dimensional model.

### 3. Results and discussion

The mean values of the IV characteristics are given in Table 1-3. The trend in  $J_{sc}$  and  $V_{oc}$  as a function of the wafer thickness is comparable for all groups.  $J_{sc}$  decreases by about 2 %;  $V_{oc}$  decreases by about 1.5 %, and the efficiency decreases by about 3.5 % relative in halving the wafer thickness. These decreases are independent of the texturing method. Note that texturing does have a tremendous effect on the output of the cells;  $J_{sc}$  increases by about 6 % while  $V_{oc}$  decreases by less than 1 %, and the cell output increases by nearly 6 % relative using the acid texture-2 compared to the NaOH etched cells (see Table 4).

**Table 1: Cell results for NaOH etched cells; errors indicate 95% confidence limit.**

Thickness ( $\mu\text{m}$ )	$J_{sc}$ ( $\text{mA}/\text{cm}^2$ )	$V_{oc}$ (mV)	Fill factor (%)	$\eta$ (%)
175	$30.8 \pm 0.8$	$598 \pm 4$	$73 \pm 2$	$13.4 \pm 0.5$
200	$30.8 \pm 0.5$	$601 \pm 2$	$72 \pm 1$	$13.4 \pm 0.3$
225	$31.1 \pm 0.5$	$600 \pm 2$	$73 \pm 1$	$13.6 \pm 0.3$
250	$31.5 \pm 0.4$	$603 \pm 2$	$73 \pm 1$	$13.9 \pm 0.2$
275	$31.7 \pm 0.4$	$605 \pm 2$	$73 \pm 1$	$13.9 \pm 0.2$
300	$31.6 \pm 0.5$	$605 \pm 2$	$73 \pm 1$	$13.8 \pm 0.3$
325	$31.2 \pm 0.6$	$607 \pm 3$	$71 \pm 2$	$13.7 \pm 0.3$

**Table 2: Cell results for acid texture-1 cells; errors indicate 95% confidence limit.**

Thickness ( $\mu\text{m}$ )	$J_{sc}$ ( $\text{mA}/\text{cm}^2$ )	$V_{oc}$ ( $\text{mV}$ )	Fill factor (%)	$\eta$ (%)
175	32.5 $\pm$ 0.6	595 $\pm$ 2	73 $\pm$ 2	14.2 $\pm$ 0.6
200	32.1 $\pm$ 0.6	593 $\pm$ 2	71 $\pm$ 2	13.5 $\pm$ 0.6
225	32.6 $\pm$ 0.9	597 $\pm$ 4	74 $\pm$ 3	14.4 $\pm$ 0.9
250	32.3 $\pm$ 0.5	598 $\pm$ 2	73 $\pm$ 2	14.1 $\pm$ 0.5
275	33.0 $\pm$ 0.5	598 $\pm$ 2	74 $\pm$ 2	14.6 $\pm$ 0.5
300	32.8 $\pm$ 0.5	600 $\pm$ 2	74 $\pm$ 2	14.7 $\pm$ 0.5
325	32.9 $\pm$ 0.6	603 $\pm$ 2	73 $\pm$ 2	14.5 $\pm$ 0.6
350	33.0 $\pm$ 0.9	602 $\pm$ 4	72 $\pm$ 3	14.3 $\pm$ 0.9

**Table 3: Cell results for acid texture-2 cells; errors indicate 95% confidence limit.**

Thickness ( $\mu\text{m}$ )	$J_{sc}$ ( $\text{mA}/\text{cm}^2$ )	$V_{oc}$ ( $\text{V}$ )	Fill factor (%)	$\eta$ (%)
175	32.7 $\pm$ 0.8	592 $\pm$ 4	71 $\pm$ 4	13.7 $\pm$ 0.8
225	33.0 $\pm$ 0.8	599 $\pm$ 4	74 $\pm$ 2	14.6 $\pm$ 0.8
250	33.2 $\pm$ 0.8	599 $\pm$ 4	74 $\pm$ 2	14.7 $\pm$ 0.8
275	33.5 $\pm$ 0.8	598 $\pm$ 4	74 $\pm$ 2	14.6 $\pm$ 0.8
300	33.6 $\pm$ 0.8	601 $\pm$ 4	74 $\pm$ 2	14.6 $\pm$ 0.8
350	33.7 $\pm$ 0.8	602 $\pm$ 4	71 $\pm$ 4	14.4 $\pm$ 0.8

**Table 4: Changes in cell parameters relative to the NaOH etched group.**

	$J_{sc}$	$V_{oc}$	$J_{sc} \times V_{oc}$	FF	$\eta$
NaOH	1	1	1	1	1
acid texture-1	1.04	0.992	1.03	1.01	1.04
acid texture-2	1.06	0.992	1.05	1.00	1.06

It is found that the IQEs only depend on the wafer thickness and are practically independent of the front side texturing. Only a small difference is found in the blue response which is even slightly higher for the acid textured cells compared to the NaOH etched cells. At 400 nm the IQE of the acid etched wafers is about 78 $\pm$ 1 % compared to 74 $\pm$ 2 % for the NaOH etched cells, irrespective of the wafer thickness. From PC1D modelling, this can be explained by a variation in the effective front surface recombination velocity ranging from 1 $\cdot$ 10<sup>5</sup> to 3 $\cdot$ 10<sup>5</sup> cm/s.

Figure 2 shows the ratio of the IQE for the various wafer thicknesses relative to the IQE of the 325  $\mu\text{m}$  wafer for the acid texture-1 scenario. From this figure, 3 regions can be distinguished: i) wavelengths shorter than about 850 nm for which the IQE is practically independent of the wafer thickness, ii) wavelengths between 900 and 1025 nm where the IQE of wafers seem to split into two groups: wafer thickness < 250  $\mu\text{m}$  and wafer thickness  $\geq$  250  $\mu\text{m}$ , and iii) wavelengths over 1050 nm where a continues decrease in IQE with decreasing wafer thickness is observed.

To explain the behaviour at wavelengths above 900 nm, a PC1D parameter set has been developed which fits the IQE,  $J_{sc}$  and  $V_{oc}$  simultaneously for all the wafer thickness within a group. Because it was not possible to model the front side texturing in PC1D we used the measured reflection curve as an input parameter instead of a front side coating. PC1D distinguishes between the front surface reflection and the front surface escape, the latter being the light reflected at the rear surface and leaving the cell through the front surface. The experimental curve is the sum of the front surface reflection and the front surface escape. The front surface reflection curve at wavelengths above 1000 nm was therefore estimated by linear extrapolation of the experimental reflection curves. To fit the  $V_{oc}$  to the experimental values, a shunting diode with diode factor 2 was used in the PC1D model. The saturation current of this diode had to be increased for the acid etched cells compared to the NaOH etched cells. As a starting point for modelling the bulk lifetime, the rear side recombination and the rear side internal reflection, the results of our previous modelling [4] has been used.

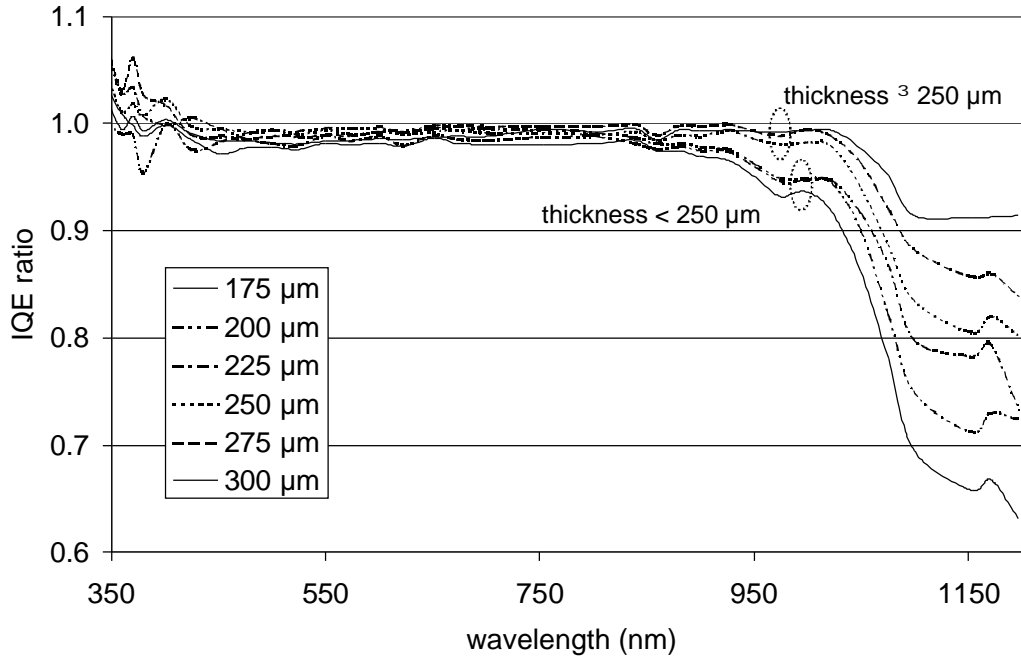


**Figure 2: IQE ratio relative to the 325  $\mu\text{m}$  thick wafer for acid texture-1 group**

Because of the observed differences in behaviour of the IQE between 900 and 1025 nm and above 1050 nm, special attention has been given in the modelling to these regions. The dependence of the IQE on the wafer thickness at 1000 nm was used as typical for the region of 900 to 1025 nm, while the IQE at 1100 nm was used as typical for the region above 1050 nm. The optimisation of the parameter set is performed in an iterative process. First optimising the bulk diffusion length to fit the trends in the IV characteristics, second optimise the effective rear recombination velocity to fit the trend in IQE at 1000 nm, third fit the internal rear reflection by fitting the trend in IQE at 1100 nm. This procedure was repeated until a consistent parameter set was obtained for all cells.

In Figure 3 the IQE at a wavelength of 1000 nm is shown for all texturing scenarios as a function of the wafer thickness. Also shown are some lines calculated using PC1D for different values of  $S_{\text{eff, rear}}$ . For all groups a drop in  $S_{\text{eff, rear}}$  is observed for wafers thinner than 250  $\mu\text{m}$ . We believe that this is related to the firing conditions used. To prevent the thinner wafers from being overfired, they were fired at a lower set-point in combination with a lower belt speed. The ramp-up rate of the thinner wafers was 70°C/s, compared to 90°C/s for the thicker wafers as measured with the Datapaq system. These conditions are based on our experience in firing 200  $\mu\text{m}$  thin wafers. The different ramp up rate resulted in an  $S_{\text{eff, rear}}$  of about 1550 cm/s for the thicker wafers ( $\bullet$  250  $\mu\text{m}$ ), and increases to about 2000 cm/s for the thinner wafers (<250  $\mu\text{m}$ ). This corresponds to the results of Narasimha et al [8] who showed for Fz wafers and RTP processing that lowering the ramp-up during the alloying of an Al-BSF results in a decrease of  $S_{\text{eff, rear}}$ .

Figure 4 shows the decrease in IQE at a wavelength of 1100 nm with wafer thickness. Also shown are PC1D calculations of the IQE for a rear side internal reflectance ( $\text{Refl}_{\text{rear}}$ ) of respectively 77.5 %, 76 % and 74.5 % (solid lines). From this figure it is clear that a good description of the decrease in IQE is obtained with  $\text{Refl}_{\text{rear}} = 76$  %, irrespective of the front side texturing. This value is in good agreement with the value of 78 % obtained before from modeling of the reflectance of polished 50  $\mu\text{m}$  thin samples [4].

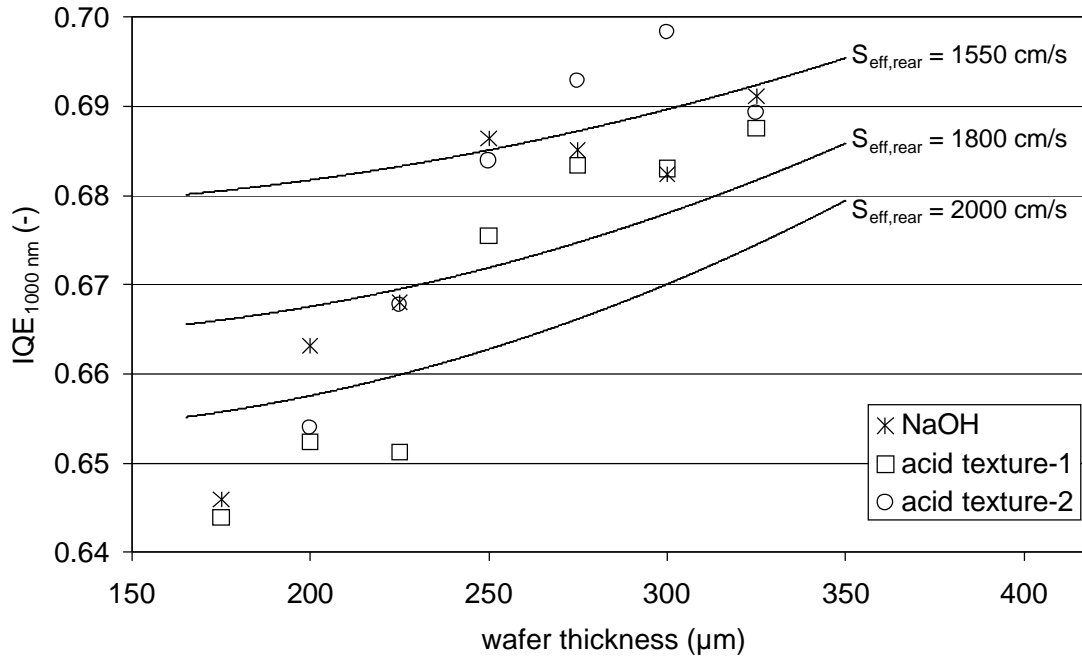


**Figure 3: IQE at a wavelength of 1000 nm as function of the wafer thickness. Solid lines are calculated with PC1D using rear reflectivity of 76 % and  $S_{\text{eff, rear}}$  of 1550 cm/s, 1800 cm/s, and 2000 cm/s respectively.**

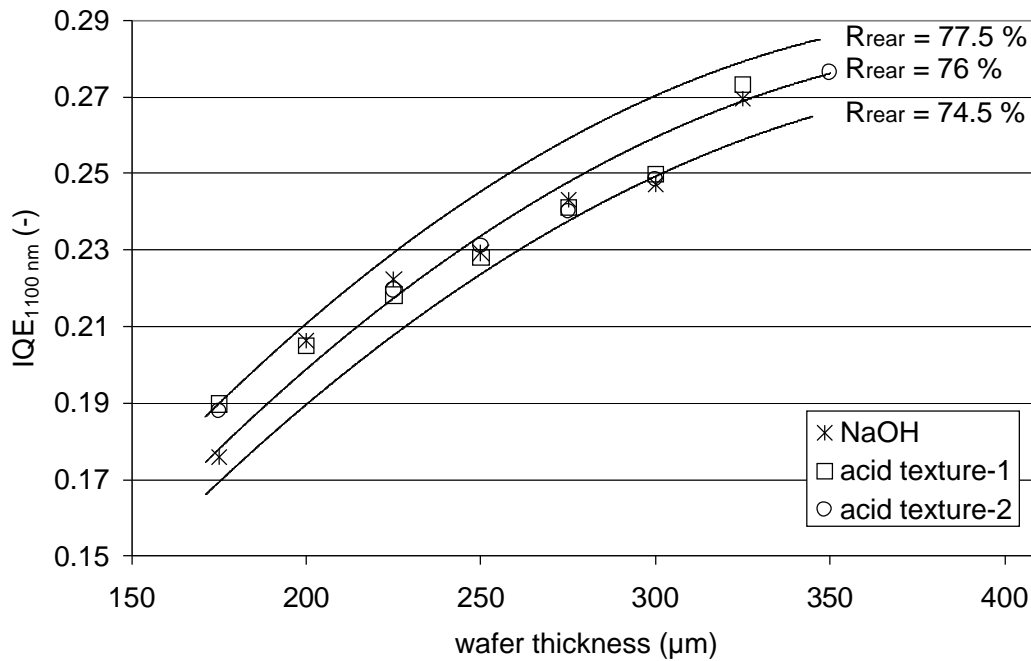


**Figure 4: IQE at a wavelength of 1100 nm as a function of the wafer thickness. Lines are calculated with PC1D using  $\text{Refl}_{\text{rear}}$  is 74.5 %, 76 % and 77.5 % respectively and  $S_{\text{eff, rear}} = 1550$  cm/s and 2000 cm/s.**

The trends in  $J_{\text{sc}}$  and  $V_{\text{oc}}$  versus wafer thickness are shown in Figure 5 and Figure 6 respectively. The lines are calculated with PC1D. The bump in the lines result from the use of different  $S_{\text{eff, rear}}$  for wafers with thickness  $< 250 \mu\text{m}$  or  $\geq 250 \mu\text{m}$  as explained in Figure 3. In Figure 6 only one line is

shown for the modeled  $V_{oc}$  of the acid textured cells because  $V_{oc}$ s estimated for the two textures differ by less than 1 mV over the whole thickness range.

The fits show good correspondence with the wide distribution of the experimental data. So the PC1D model can be used to predict the efficiencies for different situations. We discuss with more detail i) the reason for the efficiency loss solely due to the wafer thickness; ii) the origin of the  $V_{oc}$  drop in the acid textured cells compared to the NaOH etched cells, and iii) the influence of the material quality on the efficiency distribution when thinner wafers are used.

The PC1D model reveals that halving the wafer thickness from 350 to 175  $\mu\text{m}$  should result in a 3 % loss in  $J_{sc}$  and a 1 % loss in  $V_{oc}$  taking into account the difference in rear surface passivation of the two thicknesses. About one third of the losses in  $J_{sc}$  and  $V_{oc}$  can be attributed to the difference in rear surface passivation of the thin and thick cell. Assuming  $S_{eff, rear} = 1550 \text{ cm/s}$  in both cases, the estimated losses in  $J_{sc}$  and  $V_{oc}$  are only 2 % and 0.6 % respectively. These remaining losses result from the imperfect of  $S_{eff, rear}$  and  $R_{rear}$ . They are independent of the front surface texturing.

Figure 6 shows that the  $V_{oc}$  of the acid textured cells is about 5 mV lower compared to the NaOH etched cells. Meemongkolkiat et al. [9] explained the drop in  $V_{oc}$  of textured cells made of Cz material by an increased rear surface recombination velocity. However, we showed that for our cells the rear surface recombination velocities are comparable for NaOH etched and acid textured cells. The IQE measurements revealed that it is also not the front surface recombination velocity which decreases the  $V_{oc}$ ; the blue response was even slightly higher for the acid etched cells than for the NaOH etched cells. We believe that the decrease in  $V_{oc}$  results from an increased recombination near the depletion region, maybe as a result of the increased area of the depletion region. In the PC1D model, the saturation current of the shunting diode had to be increased slightly for the acid etched cells compared to the NaOH etched cells.

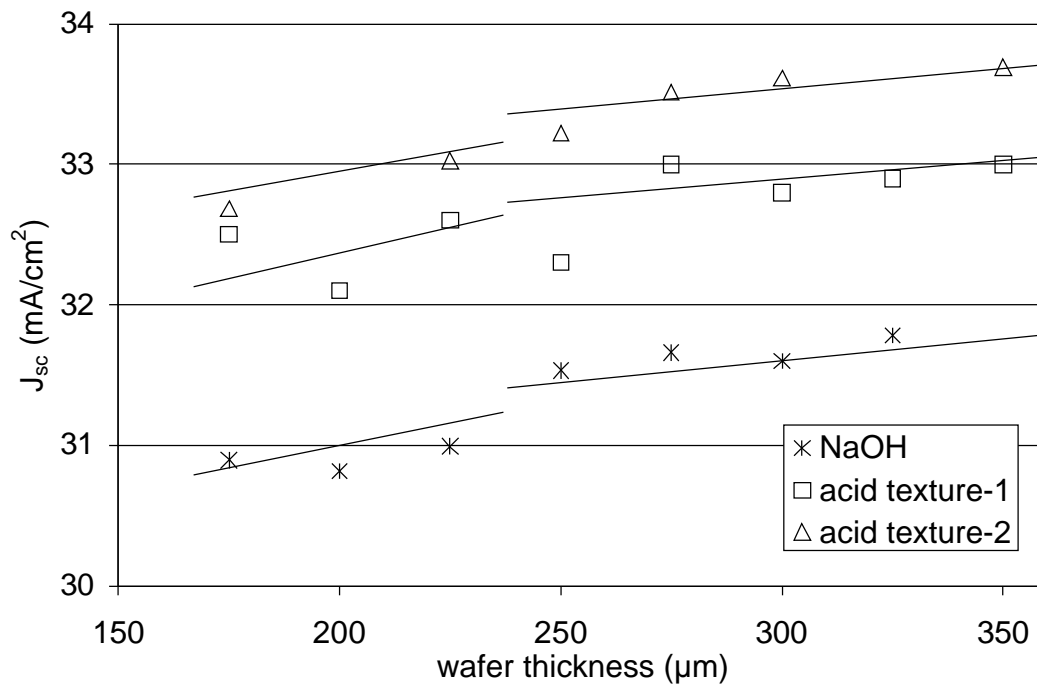


**Figure 5: Influence of wafer thickness on  $J_{sc}$ . Solid lines are calculated with PC1D using  $S_{rear, eff}$  of 1550 and 2000  $\text{cm/s}$  for wafers  $\geq 250 \mu\text{m}$  and wafer  $< 250 \mu\text{m}$  respectively and  $\text{Refl}_{rear}$  of 76 %.**

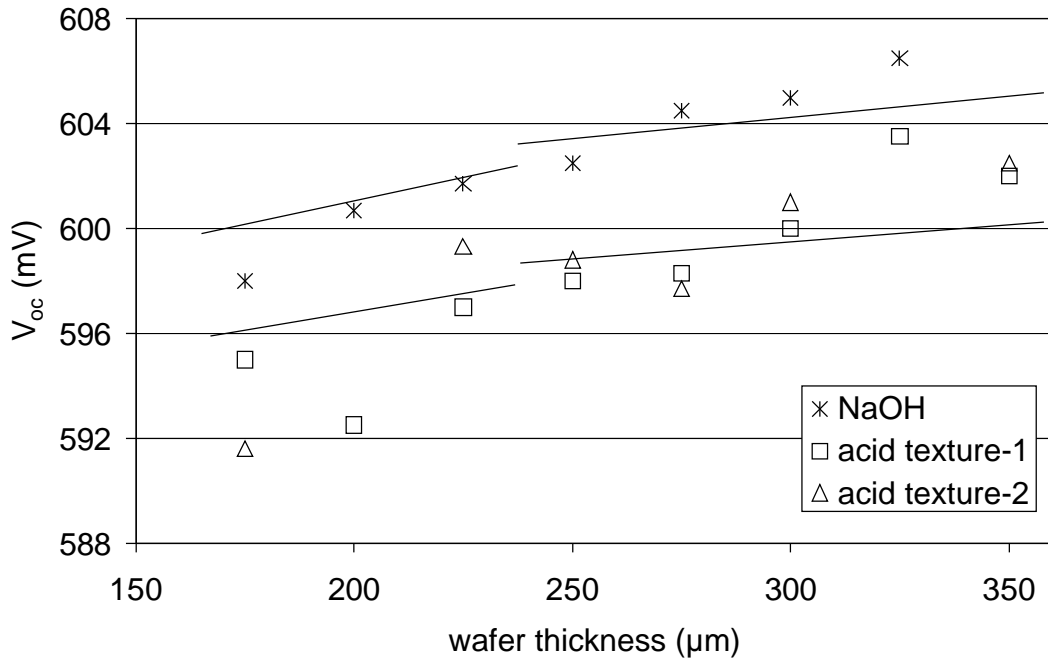


**Figure 6: Influence of wafer thickness on  $V_{oc}$ . Lines are calculated with PC1D using  $S_{rear,eff}$  of 1550 and 2000 cm/s for wafers  $\geq 250 \mu\text{m}$  and wafer  $< 250 \mu\text{m}$  respectively and  $Refl_{rear}$  of 76 %.**

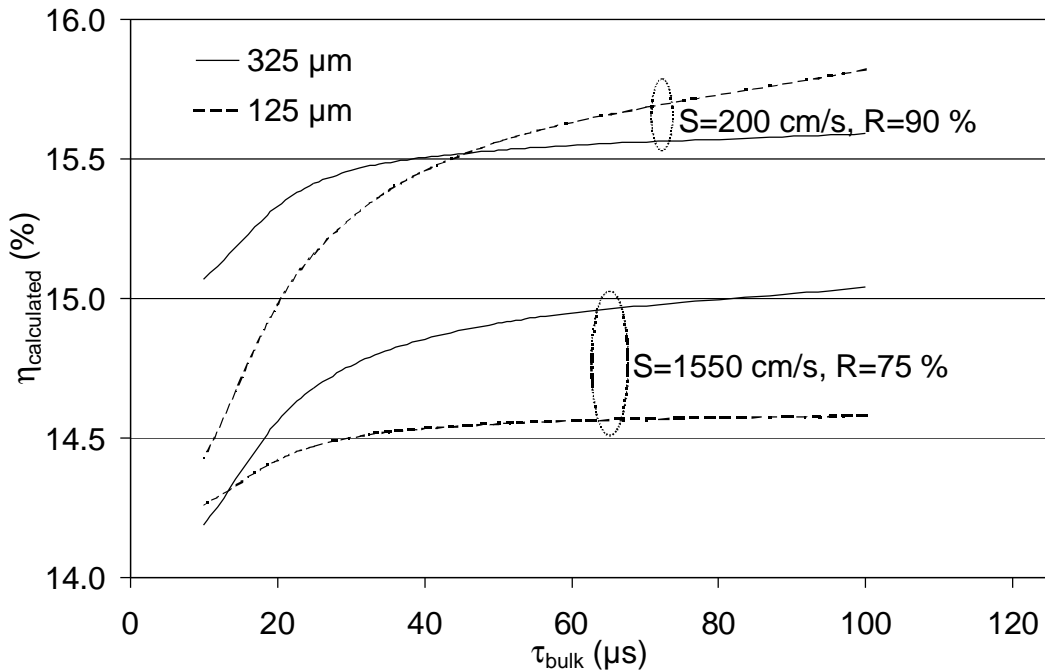


**Figure 7: Influence of the material quality on the efficiency for thin and thick wafers calculated with  $S_{eff,rear} = 1550 \text{ cm/s}$  and  $Refl_{rear} = 76 \%$ .**

Figure 7 shows the calculated efficiency as a function of the materials quality for two wafer thicknesses and rear sides with two different property sets. In these calculations the difference in  $S_{eff,rear}$  due to the different firing is neglected. Typically for normal multi crystalline material,  $\tau_{bulk}$  varies between 10 and 100  $\mu\text{s}$ . Although the efficiency distribution is much smaller for the thin

wafers, the efficiency is about 0.5 % absolute lower for the processing scheme used which realised  $S_{\text{eff, rear}}=1550$  cm/s and  $R_{\text{rear}}=75$  %. When a processing scheme could be used that improves the rear side ( $S_{\text{eff, rear}} = 200$  cm/s;  $R_{\text{rear}} = 90\%$ ) without effecting the bulk and the front side the reduction in efficiency distribution is even better. At the same time, the average efficiencies for the thin and thick cells are comparable.

Also shown by Figure 7 is that the experimentally obtained loss in  $J_{\text{sc}}$  and  $V_{\text{oc}}$  is not only influenced by the properties of the rear side, but also by the bulk of the wafer. For wafers with a low  $\tau_{\text{bulk}}$  ( $< 10$   $\mu\text{s}$ ), the losses are negligible, or even an efficiency gain can be obtained.

#### 4. Conclusions

The influence of the wafer thickness on the trends in IV characteristics is independent of the front side texturing when an optimised SiN AR coating is used. Halving the wafer thickness results in a 3 % loss in  $J_{\text{sc}}$  and a 1.5 % loss in  $V_{\text{oc}}$ . About one third of the losses result from differences in the rear side recombination velocity between the thicker and the thinner cells due to the different firing conditions used. The remaining loss of about 2.5 % relative in efficiency results from both the imperfect rear surface reflection and the finite rear surface recombination velocity. These effects are independent of the front surface texturing.

The decrease in  $V_{\text{oc}}$  for the acid etched wafers compared to the NaOH etched wafers does not result from an increased surface recombination velocity neither front nor rear, but probably result from an increased recombination near the depletion region.

The rear surface recombination velocity is independent of the texturing method, but it does depend on the firing profile used. A higher ramp-up rate results in a decrease of the recombination velocity.

The use of thinner wafers will narrow the efficiency distribution, and will give a higher efficiency gain when better rear surface passivation schemes are introduced.

Acid texturing results in about a 6 % increase in  $J_{\text{sc}}$  and about a 1 % decrease in  $V_{\text{oc}}$  compared to NaOH etched cells, independent of the wafer thickness.

#### ACKNOWLEDGEMENTS

This work was carried out by ECN as part of the TOPSICLE project funded by the European Commission's FP5 Energie R&D programme (contract no. ENK6-CT2002-00666).

#### REFERENCES

- [1] T.M. Bruton, S.R. Roberts, R.W. Russell, W. Warta, S. Glunz, W. Koch, A. Luque, R. Lago, L.J. Caballero, C. Del Ca• izaro, A. Marti, L. Frisson and A. Vallera, Proc. 17<sup>th</sup> European PV SEC, 2001, 1282-1286.
- [2] S. Steckemetz, A. Metz and R. Hezel, Proc. 17<sup>th</sup> European PV SEC, 2001, 1902-1905
- [3] W. Warta, S.W. Glunz, J. Dicker and J. Knobloch, Prog. Photovolt: Res. Appl., 2000, **8**, 465-471
- [4] C.J.J. Tool, A.R. Burgers, P. Manshanden, A.. Weeber, and B.H.M. van Straaten, Prog. Photovolt: Res. Appl., 2002, **10**, 279-291
- [5] J. Hoornstra, A.S.H. van de Heide, J.H. Bultman and A.W. Weeber, Proc. PV in Europe, Rome 2002, 276-279.
- [6] www.statgraphics.com (December 2003).
- [7] P.A. Basore and D.A. Clugston, Proc. 25<sup>th</sup> IEEE PVSC 1996, 377-381.
- [8] S. Narasimha, A. Rohatgi and A.W. Weeber, IEEE Trans, Electron. Devices, 1999, **46**(7), 1363-1369.
- [9] V. Meemongkolkiat, M. Hilali and A. Rohatgi, Proc. 3<sup>rd</sup> World Conference PVSEC, Osaka, 2003.